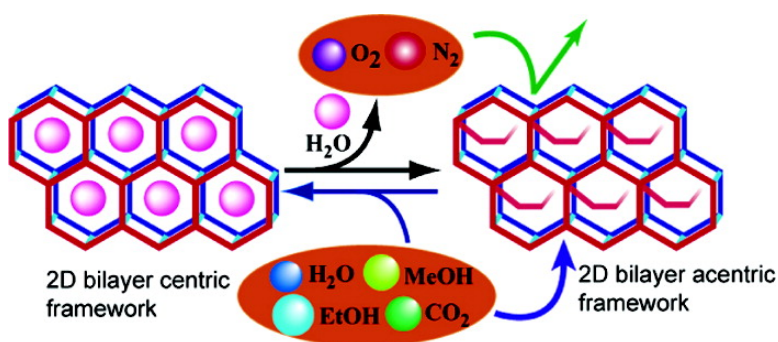


Guest-Induced Asymmetry in a Metal–Organic Porous Solid with Reversible Single-Crystal-to-Single-Crystal Structural Transformation

Tapas Kumar Maji, Golam Mostafa, Ryotaro Matsuda, and Susumu Kitagawa

J. Am. Chem. Soc., **2005**, 127 (49), 17152-17153 • DOI: 10.1021/ja0561439 • Publication Date (Web): 17 November 2005

Downloaded from <http://pubs.acs.org> on March 25, 2009



More About This Article

Additional resources and features associated with this article are available within the HTML version:

- Supporting Information
- Links to the 37 articles that cite this article, as of the time of this article download
- Access to high resolution figures
- Links to articles and content related to this article
- Copyright permission to reproduce figures and/or text from this article

[View the Full Text HTML](#)



Guest-Induced Asymmetry in a Metal–Organic Porous Solid with Reversible Single-Crystal-to-Single-Crystal Structural Transformation

Tapas Kumar Maji,[†] Golam Mostafa,[‡] Ryotaro Matsuda,[†] and Susumu Kitagawa^{*,†}

Department of Synthetic Chemistry and Biological Chemistry, Graduate School of Engineering, Kyoto University, Katsura, Kyoto 615-8510, Japan, and Department of Physics, Jadavpur University, Jadavpur, Kolkata 700 032, India

Received September 7, 2005; E-mail: kitagawa@sbchem.kyoto-u.ac.jp

Compared to the rigid and robust metal–organic frameworks,¹ recently, there has been growing interest in flexible and dynamic frameworks, in particular, those that reversibly change their structures and properties in response to external stimuli. This so-called “structural dynamism” would be a key principle for high selectivity, accommodation, and separation of specific molecules, and at present is regarded as the basis of a new class of practical materials.^{2,3} Hence the design and synthesis of a host framework that can interact with certain guest molecules in a switchable way has implications for a generation of advanced materials, with potential applications for molecular sensing and actuators. Here we present the synthesis, structure, and sorption properties of a 2D bilayer open framework of Cu(II), $\{[\text{Cu}(\text{pyrdc})(\text{bpp})](5\text{H}_2\text{O})\}_n$ (**1**) [pyrdc = pyridine-2,3-dicarboxylate; bpp = 1,3-bis(4-pyridyl)-propane], which shows reversible sponge-like dynamic behavior⁴ with centric-to-acentric structural transformation upon dehydration–rehydration with retention of single crystallinity. The dehydrated nonporous framework shows a gate-opening phenomenon⁵ for selective adsorbates at a certain vapor pressure, concomitant with a structural transformation to a porous phase correlated with the hydrogen-bonding interactions.

The framework $\{[\text{Cu}(\text{pyrdc})(\text{bpp})](5\text{H}_2\text{O})\}_n$ (**1**) was synthesized by the reaction of $\text{Cu}(\text{NO}_3)_2$ with Na_2pyrdc and bpp in $\text{H}_2\text{O}/\text{MeOH}$ medium. The X-ray crystal structure of **1**^{6a} reveals a 2D bilayer open framework composed of one Cu(II), pyrdc, and bpp ligand in the asymmetric unit (Figure S1). The 2D layer with a honeycomb motif is composed of the $\text{Cu}(\text{pyrdc})(\text{py}-(\text{CH}_2)_3-$ of the bpp (Figure 1a), which is connected via a “pillar” composed of the pyridine (py) part of the same bpp ligand to another layer, forming the 2D pillared-bilayer structure with 3D water-filled channels (Figure 1b). The bpp ligand shows conformational flexibility along the long $-\text{CH}_2-$ chain, which is in a bending conformation with the angle, $\text{py}-\text{C}-\text{C}$ of 111.50° , and the two pyridine rings are in an *anti* conformation with a dihedral angle of $70.2(5)^\circ$. The pillar pyridine rings are regularly positioned almost parallel to the direction of the side channels (Figure 1b), and the thickness of the bilayer galleries is 14.00 \AA . The open framework has channels with dimensions of 5.5×3.7 and $2.3 \times 2.1 \text{ \AA}^2$ along the *c*- and *b*-axes, respectively, and the estimated solvent-accessible void volume is 22.8% of the total crystal volume (Figure 1a and b).^{7,8}

The TG curve of **1** indicates the release of the guest water molecules up to 85°C to give the dehydrated form **1a**, and at 190°C , the ligand molecules start to be released (Figure S2). The XRPD pattern of the dehydrated form shows that the peaks at (002) and (111) have been changed, and while some new peaks appear, as at (012), these compare to the as-synthesized framework, indicating that structural transformation occurs upon dehydration (Figure S3).

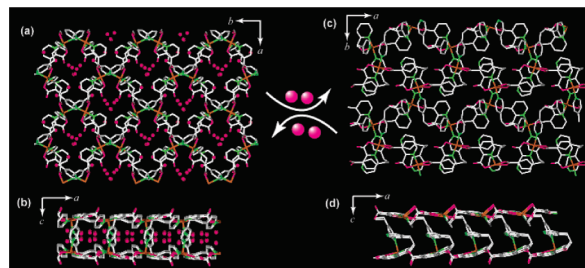


Figure 1. (a) Honeycomb-like 2D layers of **1** showing a water-filled channel along the *c*-axis. (b) Pillared-bilayer network of **1** showing the channel along the *b*-axis. (c) Honeycomb-like 2D layers of dehydrated framework, **1a** along the *c*-axis. (d) Pillared-bilayer network along the *b*-axis (the pendent bpp ligand is occupied in the channel).

However, upon exposure of **1a** to water vapor, the virgin framework regenerates (Figure S3), which is indicative of reversible crystal transformation.

To shed light on the new structure generated upon dehydration, we heated the as-synthesized blue crystal at 100°C under Ar atmosphere for 1 h. This transformed the crystal to deep blue, and single-crystal data were then collected at 100°C (Figure S4). Structure determination^{6b} reveals that, upon dehydration, **1a** crystallizes in the acentric and polar space group, $Pca2_1$ (orthorhombic), and the Flack’s parameter, $0.502(9)$, suggests a twinned racemate crystal. The cell volume decreases by 12.62%, indicating a drastic contraction of the framework. In the asymmetric unit of **1a**, there are two crystallographically independent Cu(II) ions that have the molecular formula $\{[\text{Cu}(\text{pyrdc})(\text{bpp})]_2\}_n$ (Figure S1). The most interesting aspect of the dehydrated structure is the presence of two different 2D layers (Figure 1c); one contains the Cu(1) and related atoms, while the other contains Cu(2) and related atoms, and the 2D layers are connected by the one bpp ligand to afford 2D bilayer galleries (Figure 1d). It is noteworthy that another bpp ligand is pendant and attached to the Cu(2), indicative the breaking of the Cu–N(bpp) bond, protrudes to the groove of the bilayer, such that there is no effective open space or channel (nonporous form) (Figure 1d). The thickness of the bilayer galleries is reduced to 11.88 \AA . Upon keeping the dehydrated single crystal in the open atmosphere for 1 week, we observed that the color of the crystal slowly changes from dark blue to light blue (**1b**), comparable to the as-synthesized crystal (Figure S4). X-ray structure determination of the corresponding crystal (**1b**) shows that the cell volume increases^{6c} from $3843(2)$ to $4312(5) \text{ \AA}^3$, and the space group changes to the original, $Pbcn$. The full assignment of the structure of **1b** shows that it is completely converted to the original as-synthesized framework **1** with regeneration of the Cu–N(bpp) bond, which accommodates three water molecules per Cu(II) in the pore, showing reversible structural transformation.

[†] Kyoto University.

[‡] Jadavpur University.

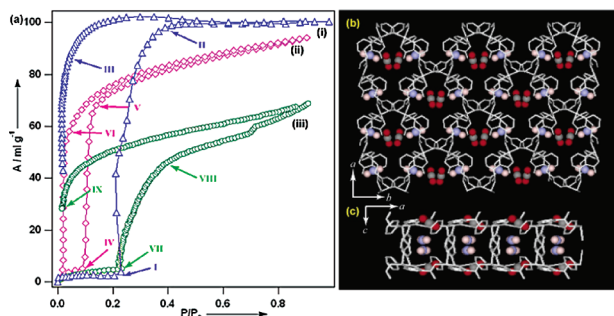


Figure 2. (a) Sorption isotherm for different adsorbate in **1a**: (i) CO₂ (195 K); (ii) MeOH; and (iii) EtOH (298 K) (where P/P_0 is the relative vapor pressure). (b) Honeycomb-like 2D layer with CO₂ molecules along the c -axis. (c) Pillared-bilayer network along the b -axis with different CO₂ molecules.

We measured the adsorption properties of the well-defined nonporous framework of **1a** with different gases (O₂, N₂, CO₂) as well as different solvents (MeOH, EtOH) to study the effect of structural transformation in other adsorbates. The adsorption isotherms for O₂ (kinetic diameter = 3.4 Å)⁹ and N₂ (3.6 Å) at 77 K reveal no inclusion by the framework, indicating that there is no porosity, as revealed by the structure determination of **1a** (Figure S5). Conversely, CO₂ (3.3 Å), regardless of its comparable size to that of O₂ and N₂, can be adsorbed, as illustrated in Figure 2a(i). The isotherm shows a sudden increase at point I (relative pressure $P/P_0 = 0.23$) and attains a saturated level at point II ($P/P_0 = 0.41$). The DR plots are almost linear in the higher-pressure region, suggesting 1.96 molecules of CO₂ are included per Cu(II) in the pore, which gives a specific surface area of 600.26 m² g⁻¹. This high specific surface area clearly shows that the nonporous phase **1a** is transformed into the microporous phase **1**. This onset pressure, at which the gates of the grooves of **1a** becomes open, is referred to as the gate-opening pressure.⁵ In contrast, the desorption isotherm does not retrace the adsorption isotherm and shows an abrupt drop at point III ($P/P_0 = 0.04$). It is very difficult to desorb all of the included CO₂, indicating a strong CO₂–host interaction (isosteric heat of adsorption of CO₂ = 32.47 kJ/mol). It is noteworthy that we have determined the crystal structure with CO₂ inclusion at –80 °C,^{6d} which shows that the honeycomb-like 2D bilayer regenerated with inclusions of CO₂ and cell volume is slightly increased compared to **1** (Figure 2b and c). Two independent CO₂ molecules in two different channels are found per Cu(II), perfectly correlating with the sorption experiment. In the pores, CO₂ molecules undergo C–H···O (2.46–2.59 Å) interaction with the channel walls, providing the driving force to the sorption with strong confinement in the framework (Figure S6) compared N₂ and O₂, exhibiting selective accommodation. A similar sorption phenomenon was observed in the case of MeOH at 298 K, and the corresponding isotherm (Figure 2a(ii)) shows a sudden increase at point IV ($P/P_0 = 0.09$) and starts to saturate at point V ($P/P_0 = 0.16$). The desorption curve does not coincide with the adsorption curve, and a sudden drop occurs at point VI ($P/P_0 = 0.03$). The lower gate-opening pressure in the case of MeOH is chiefly associated with the strong (O–H···O) hydrogen-bonding interaction with the pendent carboxylate moiety of the pyrdc ligands at the pore surface. A similar adsorption isotherm with a hysteresis profile is observed for EtOH vapor (Figure 2a(iii)) with the same gate-opening pressure as CO₂, corresponding to the large size and weaker hydrogen-bonding ability of EtOH. The prominent abrupt adsorption jump and desorption drop accompanying the large hysteresis profile for

CO₂, MeOH, and EtOH sorption correlates with the occurrence of framework transformation from a nonporous to a porous phase in the crystal state, which allows guest inclusion.

In conclusion, we have synthesized a novel 2D pillared-bilayer flexible open framework of Cu(II) using a mixed ligand system, which shows sponge-like dynamic behavior with bond breaking and bond formation triggered by guest removal and inclusion. This is the first observation of porous to nonporous phase transition of a dynamic framework, with retention of single crystallinity and introducing asymmetry into the framework upon dehydration. The selective gate-opening phenomenon with certain adsorbates is completely realized by the hydrogen-bonding interaction with apohost framework, that is, guests are permitted to pass the gate at specific gate-opening pressures that depend on the strength of the intermolecular interaction. Earlier reports hypothesizing this gate-opening and gate-closing phenomenon⁵ have now been realized with the proof provided by single-crystal structure determination.

Acknowledgment. This work was supported by Grant-In-Aid for Science Research in a Priority Area “Chemistry of Coordination Space” (No. 464) from the Ministry of Education, Science, Sports, and Culture, Japan.

Supporting Information Available: Detailed experimental procedures, TGA, IR, XRPD measurements, and photographs of the crystals and figures in different states. X-ray crystallographic files (CIF) in different states. This material is available free of charge via the Internet at <http://pubs.acs.org>.

References

- (1) (a) Kitagawa, S.; Kitaura, R.; Noro, S. I. *Angew. Chem., Int. Ed.* **2004**, *43*, 2334. (b) Yaghi, O. M.; O’Keeffe, M.; Ockwig, N. W.; Chae, H. K.; Eddaoudi, M.; Kim, J. *Nature* **2003**, *423*, 705.
- (2) (a) Kitagawa, S.; Uemura, K. *J. Chem. Soc. Rev.* **2005**, *34*, 109. (b) Bradshaw, D.; Claridge, J. B.; Cussen, E. J.; Prior, T. J.; Rosseinsky, M. *J. Acc. Chem. Res.* **2005**, *38*, 273.
- (3) (a) Serre, C.; Millange, F.; Thouvenot, C.; Nogués, M.; Marsolier, G.; Louër, D.; Férey, G. *J. Am. Chem. Soc.* **2002**, *124*, 13519. (b) Uemura, K.; Kitagawa, S.; Fukui, K.; Saito, K. *J. Am. Chem. Soc.* **2004**, *126*, 3817. (c) Maji, T. K.; Uemura, K.; Chang, H. C.; Matsuda, R.; Kitagawa, S. *Angew. Chem., Int. Ed.* **2004**, *43*, 3269. (d) Matsuda, R.; Kitaura, R.; Kitagawa, S.; Kubota, Y.; Kobayashi, T. C.; Horike, S.; Takata, M. *J. Am. Chem. Soc.* **2004**, *126*, 14063. (e) Dybtsev, D. N.; Chun, H.; Kim, K. *Angew. Chem., Int. Ed.* **2004**, *43*, 5033. (f) Halder, J. G.; Kepert, C. J.; Mobaraki, K.; Murray, K. S.; Cashion, J. D. *Science* **2002**, *298*, 1762. (g) Cussen, E. J.; Claridge, J. B.; Rosseinsky, M. J.; Kepert, C. J. *J. Am. Chem. Soc.* **2002**, *124*, 9574. (h) Biradha, K.; Hongo, Y.; Fujita, M. *Angew. Chem., Int. Ed.* **2002**, *41*, 3395. (i) Min, K. S.; Suh, M. P. *Chem.–Eur. J.* **2001**, *7*, 303. (j) Lee, E. Y.; Jang, S. Y.; Suh, M. P. *J. Am. Chem. Soc.* **2005**, *127*, 6374.
- (4) (a) Maspoeh, D.; Ruiz-Molina, D.; Wurst, K.; Domingo, N.; Cavallini, M.; Biscarini, F.; Tejada, J.; Rovira, C.; Veciana, A. *J. Nat. Mater.* **2003**, *2*, 190. (b) Suh, M. P.; Ko, J. W.; Choi, H. J. *J. Am. Chem. Soc.* **2002**, *124*, 10976. (c) Choi, H. J.; Suh, M. P. *J. Am. Chem. Soc.* **2004**, *126*, 15844.
- (5) (a) Kitaura, R.; Fujimoto, K.; Noro, S. I.; Kondo, M.; Kitagawa, S. *Angew. Chem., Int. Ed.* **2002**, *41*, 133. (b) Kitaura, R.; Seki, K.; Akiyama, G.; Kitagawa, S. *Angew. Chem., Int. Ed.* **2003**, *42*, 428. (c) Li, D.; Kaneko, K. *Chem. Phys. Lett.* **2001**, *335*, 50.
- (6) (a) Crystal data for **1**: orthorhombic, space group *Pbcn* (No. 60), $a = 14.035(5)$ Å, $b = 14.625(5)$ Å, $c = 21.424(5)$ Å, $V = 4398(2)$ Å³, $Z = 8$; $R = 0.0525$, $wR_2 = 0.1580$, GOF = 1.08. (b) Crystal data for **1a**: orthorhombic, space group *Pca2₁* (No. 29), $a = 13.732(5)$ Å, $b = 13.721(5)$ Å, $c = 20.397(5)$ Å, $V = 3843(2)$ Å³, $Z = 4$; $R = 0.0559$, $wR_2 = 0.1647$, GOF = 1.02. (c) Crystal data for **1b**: orthorhombic, space group *Pbcn* (No. 60), $a = 13.8882(10)$ Å, $b = 14.6592(12)$ Å, $c = 21.181(4)$ Å, $V = 4312.2(9)$ Å³, $Z = 8$; $R = 0.0542$, $wR_2 = 0.1332$, GOF = 1.07. (d) Crystal data with CO₂ inclusion: orthorhombic, space group *Pbcn* (No. 60), $a = 13.9126(10)$ Å, $b = 15.0856(13)$ Å, $c = 21.6595(18)$ Å, $V = 4545.9(6)$ Å³, $Z = 8$; $R = 0.0585$, $wR_2 = 0.1121$, GOF = 1.14.
- (7) The size is measured by considering van der Waals radii for constituting atoms. Hereafter, all of the size estimations of the pore are made in this way.
- (8) Spek, A. L. *PLATON*; The University of Utrecht: Utrecht, The Netherlands, 1999.
- (9) Beck, D. W. *Zeolite Molecular Sieves*; Wiley & Sons: New York, 1974.

JA0561439